Lipid Domain Depletion at Small Localized Bends Imposed by a Step Geometry

ARTICLE *in* LANGMUIR · FEBRUARY 2011

Impact Factor: 4.46 · DOI: 10.1021/la104504p · Source: PubMed

3 AUTHORS:

Matthew I Hoopes

19 PUBLICATIONS **198** CITATIONS

SEE PROFILE

Roland Faller

University of California, Davis

162 PUBLICATIONS **2,660** CITATIONS

SEE PROFILE

Marjorie L Longo

University of California, Davis

115 PUBLICATIONS **3,410** CITATIONS

SEE PROFILE

Langmuir

ARTICLE

pubs.acs.org/Langmuir

Lipid Domain Depletion at Small Localized Bends Imposed by a Step Geometry

Matthew I. Hoopes,[†] Roland Faller,[†,‡] and Marjorie L. Longo*[,†,‡]

[†]Biophysics Graduate Group, and [‡]Department of Chemical Engineering and Materials Science, University of California, Davis, California 95616, United States

ABSTRACT: Natural processes in biological cells rely on molecules to be in the right place at the right time to maintain the dynamics of living processes. When lipids in bilayer membranes move and mix, they experience kinetic and thermodynamic barriers that affect the time scales of their locations and associations with each other. One of these barriers is that of the membrane shape. Using spin coating as a deposition technique, we formed multilamellar supported lipid bilayers on topologically patterned substrates with defined step rise heights of 13 and 27 nm measured by atomic force microscopy. Each step rise imposed two ridges on the lipid bilayers, and the ridge angles were measured by atomic force microscopy. The lipid composition of this system was 1,2-dioleoyl-*sn*-glycero-3-phosphocholine (DOPC), 1,2-dipalmitoyl-*sn*-glycero-3-phosphocholine (DPPC), and cholesterol (4:4:2), doped with a fluorescent lipid, which displays liquid-ordered−liquid-disordered (L_o−L_d) phase coexistence upon cooling to 25 °C. The DPPC-rich L_o domains in the upper bilayers were established to have boundaries and positions that responded to local forces. We found that these L_o domains were depleted at the location of each step rise. We employed an equation for local bending at a ridge and demonstrate that L_o domain densities at each rise correspond to these energies. Remarkably, an energy barrier greater than $1k_BT$ is erected at a small deflection (1.3°) from planar geometry at the ridge, resulting in depletion of the majority of the optically visible L_o domains from the step rise. This work provides a means to design substrates that, in conjunction with supported lipid bilayers, provide defined localized topological energy barriers that can be used in biomembrane engineering. It also provides a method for easily analyzing the energetics of cusp-like shapes in cellular membrane structures.

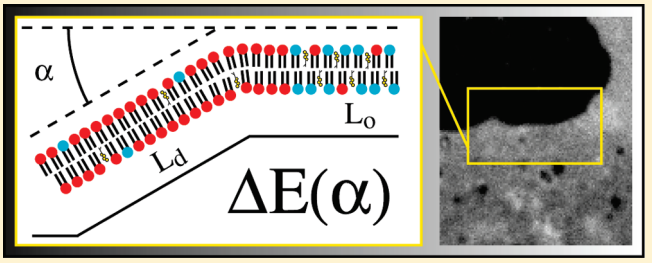

INTRODUCTION

Lipid molecules self-assemble into fluid membranes only two molecules thick to form a dual leaflet structure with fascinating properties. These dynamic assemblies not only provide for compartmentalization and transportation in the three-dimensional world of biological cells but also play a part in the organization of a two-dimensional assembly of molecules in the membrane itself. Model membrane studies have indicated that membrane curvature plays an important role in the location of lipid species in the cell. While individual molecules appear unsusceptible to curvature sorting,[1] when heterogeneous lipid compositions form in the membrane, they will localize to regions with curvatures that are energetically favorable.[2] Systems of lipids, proteins, sugars, and other biological molecules are governed by the laws of soft matter physics. Understanding the relationships between geometry, energy, and time scale in these systems is necessary for insight into how dynamic processes, such as lipid sorting, function in the cell. In addition, these insights can be used to engineer soft matter systems that use geometry to control energy and dynamics.

Similar past work shows the relationship of lateral domain organization to curvature on double-supported lipid bilayers,[3] as well as curvature sorting of lipid domains in giant unilamellar vesicles (GUVs) and microtubule-like tethers.[1] Consensus in these studies indicates that the differences in the bending stiffness of the lipid phases experiencing curvature lead to the aggregate lipid sorting behavior to lower the system energy. This means that curvature precedes the localization of specific lipid species aggregates or aggregates of classes of lipids with specific physical properties. In our work, as in past work, this property is the bending stiffness of the membrane, which can be derived directly from the area compressibility modulus, K_A,[4] of an elastic lipid bilayer.

The purpose of the present work is to offer an application of elastic theory to the deflection of adsorbed membranes and to demonstrate how this affects lipid organization of phase-separated liquid-ordered, L_o, domains surrounded by a liquid-disordered, L_d, phase. The study of supported lipid bilayers is a convenient method for analyzing the membrane because of the planar geometry. One consideration with this method is that the adsorption to the substrate will influence the membrane behavior. On the basis of changes to area compressibility, computational models have shown that single supported bilayers will have a higher bending stiffness to that of free bilayers[5] and past experimental work has used double bilayers to reduce the substrate influence on the membrane in question.[3] To address this, our work uses a multilamellar stack of bilayers, where the upper

Received: November 11, 2010
Revised: January 22, 2011

dx.doi.org/10.1021/la104504p | *Langmuir* XXXX, XXX, 000–000

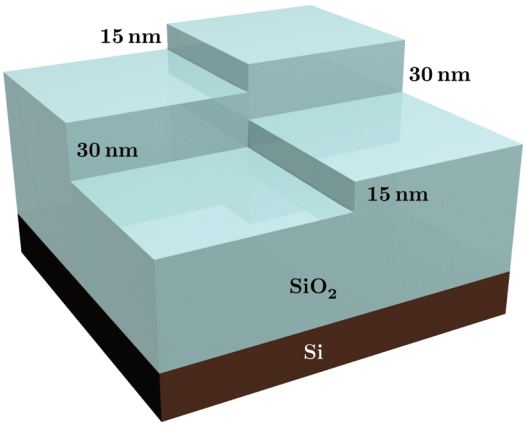

Figure 1. Illustration (not to scale) of etched features on the silicon substrates as originally designed. The orthogonal intersection of the first and second etch procedure leads to steps that cross to form steps with two different rise heights. See Figure 2 for step rise profiles.

bilayers experience diminished substrate constraints. Past work has shown that these multilamellar membranes can be made by spin-coating lipids onto a substrate, after which they are dried and subsequently rehydrated.[6−8] Our substrate is comprised of a flat SiO_2 wafer with thermal oxide into which isolated steps of two rise heights have been etched. This leaves large regions of unperturbed membrane (zero curvature) on the samples against which the effects of localized bending at the ridges, associated with the step rises, can be gauged. This geometry compliments past work by Tian and Baumgart,[1] Heinrich et al.,[2] and Parthasarathy et al.[3] with the continuous curvature of GUVs/microtubules and with repeating substrate corrugations. With this substrate, we show, using fluorescence microscopy, that localized bending of a flat membrane leads to a ridge energy, which selectively controls lipid composition near the ridge.

MATERIALS AND METHODS

Figure 1 illustrates the original lithographically patterned substrate geometry design. Substrates were prepared in the Northern California Nanotechnology Center at University of California, Davis from 4 in. (100) silicon wafers with a 1000 Å oxide layer (Silicon Quest International, Santa Clara, CA). A mask was designed using Ledit software (Tanner Research, Monrovia, CA) for a 5 in. mask that was created on a Mann 3600 pattern generator (D.W. Mann/GCA Corp., Burlington, MA). The wafer was cleaned with isopropyl alcohol and methylene chloride and then vacuum-baked at 100 °C for 15 min. The wafer was then primed with hexamethyldisilazane (HMDS) that was applied while spinning at 1000 rpm for 20 s and then vacuum-baked again at 90 °C for 2 min. An aliquot of 3 mL of SPR955-CM_0.7 resist (Dow Chemical Company, Midland, MI) was applied to the wafer on a Solitec spin coater (Solitec Wafer Processing, Inc., Milpitas, CA), spun first at 300 rpm for 15 s, followed by 2000 rpm for 45 s, and immediately treated with a soft bake at 90 °C for 45 s. A MA4 mask aligner [Karl-Suss (Suss MicroTec), Garching, Germany] was used to expose the resist. The mask was exposed using a high-pressure mercury lamp for 3.5 s at 22 mW/cm^2. Mask exposure was followed by a post-exposure bake at 110 °C for 90 s. The resist was developed with CD-26 (Shipley, Marlborough, MA) for 1 min, followed by a hard bake for 60 min at 80 °C. Reactive ion etching (RIE) of the wafer was performed with a Technics 800 using CF_4 at 10 standard cubic centimeters per minute (sccm) and a power and pressure setting of 200 W and 110 mTorr, respectively, for a duration of 15 s. Resist was stripped with PRS-3000

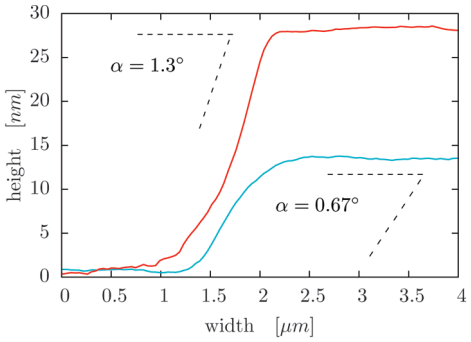

Figure 2. AFM line scan profiles for small (cyan) and large (red) step rises. Ridge angles (α) are in degrees.

(Mallinckrodt Baker, Phillipsburg, NJ). The masking, etching, and stripping process was repeated a second time with the mask pattern rotated 90°, and the RIE time increased to 75 s. Finally, substrates were diced on a Micro Automation M1006 dicing saw. The etch depths and oxide layer thickness were profiled with a Nanospec interferometer (Nanometrics, Milpitas, CA) and an I-Elli2000 imaging ellipsometer (Nanofilm Technologies, Göttingen, Germany), and the step heights were measured with a Dimension 3100 atomic force microscope (AFM) (Veeco Metrology, Inc., Santa Barbara, CA) using contact mode scans.

The protocol for spin-coating lipids outlined by Simonsen and coworkers[7,8] was used. Stock 1,2-dioleoyl-*sn*-glycero-3-phosphocholine (DOPC), 1,2-dipalmitoyl-*sn*-glycero-3-phosphocholine (DPPC), and cholesterol were used as purchased in chloroform (10 mg/mL) from Avanti Polar Lipids, Inc. (Alabaster, AL) and were combined in a 2 mL glass conical microvial in a total molar ratio of 4:4:2 DOPC/DPPC/cholesterol. To this was added the fluorescent lipid, 1-palmitoyl-2-[6-[(7-nitro-2−1,3-benzoxadiazol-4-yl)amino]hexanoyl]-*sn*-glycero-3-phosphocholine (NBD-PC, 16:0), from Avanti Polar Lipids, Inc., so that its concentration was 0.005 mol fraction of the lipid with the lower T_m (in this case, the DOPC). This mixture was then evaporated under a stream of nitrogen while vortexing to coat the sides of the vial with lipids. The solvent for spin coating was 97:3 (v/v) hexane/methanol. The goal of this solvent is that it completely dissolves the lipids at the desired concentration and still wets the substrate. The molar concentration of the lipids in this spin-coating solvent determines the number of bilayers in the multilamellar stack upon rehydration of the sample. We used a volume of hexane/methanol necessary to produce a 7 mM solution based on the total moles of lipids. The spin coater was set for 3000 rpm and 40 s, which we placed in an area free from drafts. The lithographically patterned substrate was then attached to the vacuum chuck. For a sample of 10 mm in diameter, about 20−25 μL of the lipid solution was dispensed. The solution was quickly dispensed to wet the entire substrate, and the spin coater was immediately started. After the spin coater stopped, the sample was placed in a vacuum chamber to remove solvent for 24 h. Each dry sample was then transferred to a buffer bath (10 mM Tris-HCl, 150 mM NaCl, and 2 mM $CaCl_2 \cdot H_2O$ at pH 7.4) at 70 °C, held for 30 min, and then cooled to 25 °C over 4 h in an oven (Torrey Pines Scientific, San Marcos, CA). Finally, the samples in buffer were removed from the oven and imaged with a 60× water immersion lens on a Nikon TE400, using a FITC filter set (Chroma Technology, Bellows Falls, VT), and ImageJ/Micromanager software.[9,10]

RESULTS

The lithographic fabrication process for the substrate does not create features with perfectly anisotropically etched step sides as schematically depicted in Figure 1. Rather, imperfections in the mask thickness and mask undercutting lead to step rises with a slope that deviates from vertical. Figure 2 shows AFM line scan

dx.doi.org/10.1021/la104504p |*Langmuir* XXXX, XXX, 000–000

profiles for both step rises, giving rise heights of 27 and 13 nm for the large and small rises, respectively. Rise widths from these scans yield 1160 and 1090 nm for the large and small rises, respectively. Therefore, the corners of these steps do not form right angles. Instead, they form much shallower angles characterized by a ridge angle, α, which is the deviation from completely flat (0°). The ridge angles are approximately α = 1.3° and 0.67° for the large and small step rises, respectively, as shown in Figure 2.

DOPC/DPPC/cholesterol (4:4:2) multibilayers doped with the fluorescent lipid, NBD-PC, 16:0, were deposited onto the lithographically patterned substrates and observed by fluorescence microscopy. L_o phase separated DPPC-rich domains that overlapped with each other in different bilayers of the multibilayer stack appeared as the darkest regions (as seen in Figures 3−5), as Jensen et al.[8] previously observed. Fluorescence additivity between bilayers led to a lighter shade of gray (again, see Figures 3−5) for L_o domains that did not overlap between bilayers. The regions between L_o domains were occupied by the DOPC-rich L_d phase, enriched in the fluorescent lipid.

We initially established that L_o domain boundaries were deformable in the upper lipid bilayers of this multibilayer stack system, as observed in past work.[7,8] For example, we show two images taken 13 s apart where the thin L_d region at the location indicated by the arrows separating two L_o domains disappears as the domains merge (Figure 3). The domain boundary of the elongated L_o domain on the right changes position significantly because of the merger. Additionally, large-scale motion of individual L_o domains was occasionally observed. For example, Figure 4 shows a sequence in which the motion of a small dark L_o domain (≈1 μm wide) is correlated with the motion of an overlapping L_o domain (≈3 μm wide). An arrow tracks this motion as the large domain merges with another very large domain and shows that the small domain has moved almost 3 μm in 32 s. In these cases, the L_o domain boundaries and positions moved in response to local changes and their associated forces.

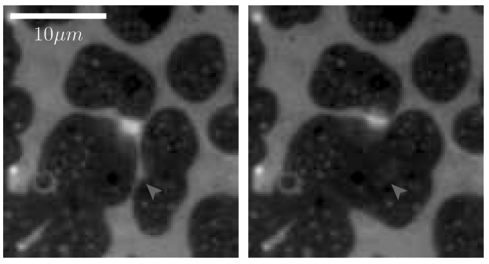

Figure 3. Deformability of L_o phase domain boundaries in an upper lipid bilayer is demonstrated in merging L_o domains (at the arrow location) and the distinct change in the shape of the domain boundary of the right-hand merging domain. The image on the right was acquired 13 s after the image on the left. The lipid bilayer composition used in this work is 4:4:2 DOPC/DPPC/cholesterol and displays L_o−L_d phase coexistence at 25 °C.

Next, we observed phase-separated DOPC/DPPC/cholesterol upper lipid bilayers, as demonstrated in Figure 5, at the location of lithographically patterned steps (Figures 1 and 2). Because of the variation in SiO_2 thickness resulting from the lithographic etch process, fluorescent lipids in the membranes on either side of a step rise each have a different brightness. This fluorescence interference contrast[11] (FLIC) aids in the location of each step. We initially observed that the distribution of phase-separated L_o domains was noticeably different at the location of each larger (27 nm) step rise in comparison to areas tens of micrometers away from the rise. Because of this, each larger step rise obviously disrupted the continuity of the L_o domain distribution, as shown in Figure 5. However, a disruption to the L_o domain distribution at the location of each smaller (13 nm) step rise was not obviously present. Figure 5 shows an image demonstrating that the smaller step rise (running from top to bottom) and larger step rise (running from left to right) influence the domain distribution differently. L_o domains cross over a significant fraction of the small rise, while they appear to cross over very little of the large rise.

To aid in distinguishing the behavior of the L_o domains on the larger and smaller step rises, we converted Figure 5 and similar micrographs to binary images and calculated a domain density factor for each row or column of pixels in the image. These profiles from analyzing Figure 5 are shown in Figure 6, where a value of 1 indicates that a L_o phase domain overlapped a pixel location in one or more of the bilayers and a value of 0 indicates that all pixel locations were in the L_d phase rich in the fluorescent lipid. The dashed vertical line indicates the location of the step rise and corresponds to the indices at the edges of Figure 5. The density factors at the step rise locations were calculated for several samples with large and small rises, and it was found that a *t* test distinguished between the means (0.16 ± 0.05 for the large rise and 0.36 ± 0.01 for the small rise) with a probability of 97%. As expected given the L_o/L_d ratio, the mean domain density factor using all locations on these samples was 0.54 ± 0.09. In comparison, significant depletion of L_o domains took place on the larger step rises, with an average domain density of 0.16 along the rise. Even the smaller step rises created some depletion of L_o domains, with an average domain density factor of 0.36 along the rise, although this is not always discernible when looking casually at images such as Figure 5. Just as domain density was noticeably depleted at the locations of the larger step rises, domain density was noticeably concentrated at locations adjacent to the large step rises. This phenomena can be seen in Figures 5 and 6, where a locally high domain density can be observed to be present within tens of micrometers of each side of the large step rise. Because of this local displacement of domains by the presence of the step rises, the mean domain density factor from all sample

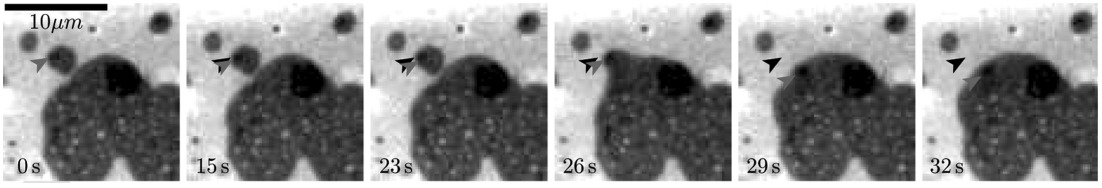

Figure 4. Small darker L_o domain in a lower lipid bilayer is mobile as it moves with a L_o domain in the lipid bilayer above.

dx.doi.org/10.1021/la104504p |*Langmuir* XXXX, XXX, 000–000

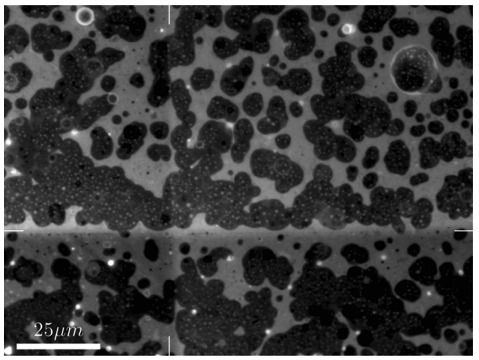

Figure 5. L_o domains are noticeably depleted at a 27 nm step rise oriented here horizontally (i.e., the rise from the two upper quadrants to the two lower quadrants is 27 nm). Also, L_o domains are less noticeably depleted at a 13 nm step rise, which is oriented vertically in the image (i.e., the rise from the two right quadrants to the two left quadrants is 13 nm). Indices on the image edges are in line with step rise locations. Brighter fluorescence indicates a lower step.

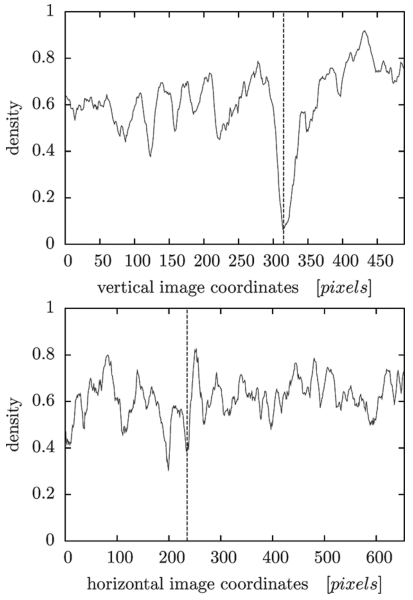

Figure 6. L_o domain density of the upper membrane averaged from horizontal and vertical line profiles in Figure 5. Pixel coordinates (0, 0) begin at the upper left of the image. The dashed vertical lines in the profile plots mark the mid-gradient contrast change at the step rise in the image using the profile tool in ImageJ.[9,10]

locations (0.54) represents the average domain density associated with a flat substrate (no step rise). Therefore, as shown in Figure 7, the L_o domain density at the rise decreased as the ridge angle associated with the rise increased from 0° (no rise) to 1.3° (large rise).

We occasionally captured large-scale collective shape rearrangement of L_o domains located at step rises that occurred on a scale of seconds. For example, in Figure 8, the shape of a domain changes significantly, such that the width of the domain spanning the small step rise increases while decreasing the perimeter of the domain. The width of the domain lobe that crosses the step increases by approximately 1 μm, while the perimeter decreases by 21 μm during the 20 s interval between the capture of the two images.

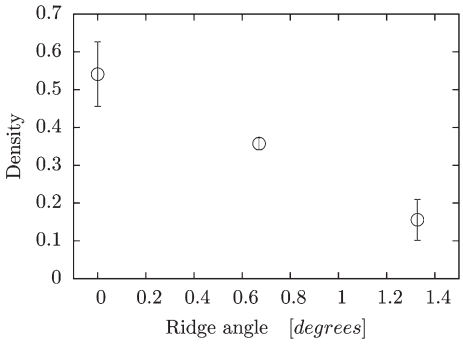

Figure 7. L_o domain density factors averaged over all locations, at the 13 nm step rises, and at the 27 nm step rises are plotted as a function of their corresponding ridge angles of 0°, 0.67°, and 1.3°, respectively.

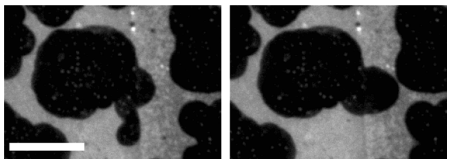

Figure 8. Two images taken 20 s apart show the movement of a L_o domain over the small step rise (10 μm scale bar).

DISCUSSION

We established in the results that L_o domain boundaries and L_o domains in the upper lipid bilayers observed here will reposition in response to local forces. Therefore, we look to the bending energy for an explanation of the observation that L_o domain density at the step rise decreased as the ridge angle of the step rise increased. Deformation of a membrane from its flat ground state shape (these phospholipids have an intrinsic curvature of zero) incurs an energy penalty. Given the aspect ratios of the step rises as we have shown above, the deflection from the lateral plane is relatively small and the adsorbed bilayer essentially makes two bends as it moves over the top ridge of the rise and then returns to its original planar orientation at the bottom ridge of the rise. The angle of deflection is small, and one can treat the required bend at each step ridge as a ridge in the bilayer.

On the basis of formulations by Lobkovsky[12] and Pomeau,[13] we use an equation for this ridge energy

$$F_{\text{ridge}} \approx K_A h^2 (L/h)^{1/3} (\alpha/2)^{7/3} \qquad (1)$$

to determine the penalty for a length of bilayer, L, to be bent at each ridge located at the step rise. Equation 1 was derived by Lobkovsky[12] by finding a separable boundary layer solution of the von Karman plate equations along a ridge line. We have assumed the small angle approximation for α (in radians). Equation 1 is identical to eq 13 by Pomeau,[13] except that we replaced Young's modulus with the well-characterized area compressibility modulus, K_A, for the two phases divided by the lipid bilayer thickness, h, from linear elastic theory. For values of K_A, we first used our original lipid mixture to determine the compositions of the individual phases using the lever rule and tie lines from published ternary-phase diagrams.[14,15] Then, we used these compositions to determine K_A for the L_d[16] and L_o[17] phases after applying corrections for apparent compressibility because of bending fluctuations.[18] This yielded K_A = 1200 mN/m for the L_o phase and K_A = 230 mN/m for the L_d phase. The L_o (DPPC

dx.doi.org/10.1021/la104504p |*Langmuir* XXXX, XXX, 000–000

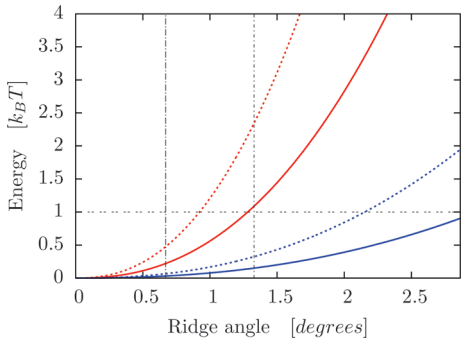

Figure 9. Plot shows ridge energy from eq 1 for a strip of membrane of width $L = 1\ \mu$m (solid) and $L = 10\ \mu$m (dashed) being bent at the ridge angles indicated for both L_o (red) and L_d (blue) phases. The bending angles of the ridges that correspond to step rises measured by AFM are marked with vertical lines, where the smaller step rise has a lower angle.

rich) and L_d (DOPC rich) phases are known to have different thicknesses,[19] and cholesterol has the effect of thinning the L_o domains[20] and thickening the L_d regions.[21] Because it is the exposure of the hydrophobic portion of the lipid that strongly contributes to K_A, we use the Gibbs−Lozzatti thickness for our calculations. Using the tabulated values from Nagle and Tristram-Nagle[19] and applying extrapolated corrections from Maulik and Shipley[20] and Nezil and Bloom,[21] we arrive at $h = 4.5$ nm for the L_o phase and $h = 3.7$ nm for the L_d phase. The ridge length parameter, L, was then selected to calculate the energy cost for a patch of membrane of that width to cross each step ridge, assuming the membrane complies with the ridge angle of the substrate. Figure 9 shows test cases for $L = 1\ \mu$m (solid) and $L = 10\ \mu$m (dashed) for both the L_o (red) and L_d (blue) phases as a function of α. The two vertical lines mark the deflection angle for the small $\alpha = 0.67°$ and large $\alpha = 1.3°$ step rises calculated from the AFM measurements.

We conclude that, for the small step rise, the difference in energy (ΔF_{ridge}) between the L_o phase and L_d phase for both ridge length values, L, chosen as examples in Figure 9 are smaller than $1k_BT$, explaining the minimal disturbance to the distribution of the L_o domains at this step rise. On the other hand, the larger step rise may allow L_o domains of 1 μm to occupy the step rise occasionally, but a L_o domain of a larger width (such as 10 μm with its $\Delta F_{ridge} \approx 2k_BT$) will have a much lower probability of crossing the rise because it exceeds thermal fluctuation energies by a factor of 2. In reality, these energies may be doubled. For example, 10 μm L_o domains or elongated L_o domains of 1 μm in width cross two ridges when they cross each step rise. Nonetheless, the reasonableness of an $\approx 1k_BT$ difference in L_o domain bending energy over the small rise versus the large rise can be gauged by a Boltzmann distribution of the L_o domain densities over the two step rises. A ratio of the L_o domain densities ($0.16/0.36 \approx 0.4$) indicates a difference in energy of $\approx 1k_BT$, validating the general approach of using eq 1 with our estimated mechanical properties. Our analysis differs from that of Parthasarathyet al.,[3] where the bending modulus difference between the two phases was approximated by setting the bending energy difference to $1k_BT$ at a critical curvature. Here, without explicit use of curvature in our equation, we have estimated the bending energy difference using the area compressibility moduli and membrane thicknesses obtained from the literature and find that the partitioning behavior is in agreement with the $\sim 1k_BT$ difference in bending energy.

Using eq 1, it can be shown that other forces at work in the membrane easily overwhelm small bending energies. The reduction in the perimeter length of the observed L_o domain in Figure 8 was about 21 μm or 28%. In this case, it appears that the energy penalty for an increased ridge length, L, was a trade off for the relaxation that occurred as a result of a decreased perimeter. Line tensions for the L_o domains are on the order of 1 pN;[22−24] therefore, the $2 \times 0.19k_BT$ increase in ridge energy to widen the part of the domain that crosses the step by 1 μm is clearly several orders of magnitude smaller than the reduction in line energy ($\Delta E \approx 21\ \mu\text{m} \times 1\ \text{pN} \approx 5000k_BT$).

This work provides a straightforward application of elastic theory to explain bending-dependent organization of lipids on patterned surfaces. It focuses on membrane bending based on deflection from a planar geometry rather than explicitly using the radius of curvature. Adsorption to the surface locally constrains bending to the ridges rather than allowing the curvature to distribute over the entire membrane. Such step patterns could be developed to create corrals of lipids species in a temperature-erasable manner, providing a way to localize chemical species on a reusable substrate as is often desired for high-throughput screening assays. Furthermore, ridge geometries appear directly in natural structures, such as in the lipid membranes surrounding the nucleocapsid in some viruses.

CONCLUSIONS

We have shown that bending in adsorbed lipid bilayers can be characterized as ridge energies. These energies lead to lateral organization of phase-separated lipids at the location of lithographically formed ridges, where the lower ridge energy of the L_d phase is favored over the L_o domains. The depletion of L_o domains at ridge locations occurred in membranes demonstrated to be fluid in the upper bilayers of a multilamellar stack. L_o domain densities on the ridge can be characterized on the basis of ridge angles, which were measured by atomic force microscopy, and we illustrated the effect of energy differences both above and below $1k_BT$. We also provided an example of forces (line tension) that are able to rearrange L_o domains to overcome organizational effects of the ridges. Further work to develop substrate patterns that further characterize shape and energy relationships in supported lipid bilayers is sure to benefit lipid membrane biophysics and engineering with this facile sample preparation platform.

AUTHOR INFORMATION

Corresponding Author
*E-mail: mllongo@ucdavis.edu.

ACKNOWLEDGMENT

Matthew I. Hoopes thanks the Northern California Nanotechnology Center (NCNC) for technical assistance during substrate fabrications. This project was supported by the National Science Foundation (NSF) Nanoscale Interdisciplinary Research Team (NIRT) Program and a National Science Foundation−International Research and Education in Engineering (NSF−IREE) international travel supplement (Grant CBET 0506602). Matthew I. Hoopes also acknowledges support by an industry/campus supported fellowship under the Training Program in Biomolecular Technology (T32-GM08799) at the University of California, Davis.

REFERENCES

(1) Tian, A.; Baumgart, T. *Biophys. J.* **2009**, *96*, 2676–2688.
(2) Heinrich, M.; Tian, A.; Esposito, C.; Baumgart, T. *Proc. Natl. Acad. Sci. U.S.A.* **2010**, *107*, 7208–7213.
(3) Parthasarathy, R.; Yu, C.; Groves, J. T. *Langmuir* **2006**, *22*, 5095–5099.
(4) Rawicz, W.; Olbrich, K. C.; McIntosh, T.; Needham, D.; Evans, E. *Biophys. J.* **2000**, *79*, 328–339.
(5) Hoopes, M. I.; Deserno, M.; Longo, M. L.; Faller, R. *J. Chem. Phys.* **2008**, *129*, No. 175102.
(6) Mennicke, U.; Salditt, T. *Langmuir* **2002**, *18*, 8172–8177.
(7) Simonsen, A. C.; Bagatolli, L. A. *Langmuir* **2004**, *20*, 9720–9728.
(8) Jensen, M. H.; Morris, E. J.; Simonsen, A. C. *Langmuir* **2007**, *23*, 8135–8141.
(9) Abramoff, M. D.; Magelhaes, P. J.; Ram, S. J. *Biophotonics Int.* **2004**, *11*, 36–42.
(10) Stuurman, N.; Amodaj, N.; Vale, R. *Microsc. Today* **2007**, *15*, 42–43.
(11) Parthasarathy, R.; Groves, J. T. *Cell Biochem. Biophys.* **2004**, *41*, 391–414.
(12) Lobkovsky, A. E. *Phys. Rev. E: Stat., Nonlinear, Soft Matter Phys.* **1996**, *53*, No. 3750.
(13) Pomeau, Y. *Philos. Mag. B* **1998**, *78*, 235–242.
(14) Marsh, D. *Biochim. Biophys. Acta, Biomembr.* **2009**, *1788*, 2114–2123.
(15) Veatch, S. L.; Soubias, O.; Keller, S. L.; Gawrisch, K. *Proc. Natl. Acad. Sci. U.S.A.* **2007**, *104*, 17650–17655.
(16) Needham, D.; Nunn, R. S. *Biophys. J.* **1990**, *58*, 997–1009.
(17) Tierney, K. J.; Block, D. E.; Longo, M. L. *Biophys. J.* **2005**, *89*, 2481–2493.
(18) Ly, H. V.; Longo, M. L. *Biophys. J.* **2004**, *87*, 1013–1033.
(19) Nagle, J. F.; Tristram-Nagle, S. *Biochim. Biophys. Acta, Biomembr.* **2000**, *1469*, 159–195.
(20) Maulik, P. R.; Shipley, G. G. *Biophys. J.* **1996**, *70*, 2256–2265.
(21) Nezil, F. A.; Bloom, M. *Biophys. J.* **1992**, *61*, 1176–1183.
(22) Baumgart, T.; Hess, S. T.; Webb, W. W. *Nature* **2003**, *425*, 821–824.
(23) Tian, A. W.; Johnson, C.; Wang, W.; Baumgart, T. *Phys. Rev. Lett.* **2007**, *98*, No. 4.
(24) Blanchette, C. D.; Lin, W.-C.; Orme, C. A.; Ratto, T. V.; Longo, M. L. *Langmuir* **2007**, *23*, 5875–5877.